Increased Hepatic PDGF-AA Signaling Mediates Liver Insulin Resistance in Obesity-Associated Type 2 Diabetes

Amar Abderrahmani, Loïc Yengo, Robert Caiazzo, Mickael Canouil, Stéphane Cauchi, Violeta Raverdy, Valérie Plaisance, Valérie Pawlowski, Stéphane Lobbens, Julie Maillet, et al.

Increased Hepatic PDGF-AA Signaling Mediates Liver Insulin Resistance in Obesity-Associated Type 2 Diabetes

Amar Abderrahmani,[1,2] Loïc Yengo,[1] Robert Caiazzo,[3] Mickaël Canouil,[1] Stéphane Cauchi,[1] Violeta Raverdy,[3] Valérie Plaisance,[1] Valérie Pawlowski,[1] Stéphane Lobbens,[1] Julie Maillet,[1] Laure Rolland,[1] Raphael Boutry,[1] Gurvan Queniat,[1] Maxime Kwapich,[1] Mathie Tenenbaum,[1] Julien Bricambert,[1] Sophie Saussenthaler,[4] Elodie Anthony,[5] Pooja Jha,[6] Julien Derop,[1] Olivier Sand,[1] Iandry Rabearivelo,[1] Audrey Leloire,[1] Marie Pigeyre,[3] Martine Daujat-Chavanieu,[7] Sabine Gerbal-Chaloin,[7] Tasnim Dayeh,[8] Guillaume Lassailly,[9] Philippe Mathurin,[9] Bart Staels,[10] Johan Auwerx,[6] Annette Schürmann,[4] Catherine Postic,[5] Clemens Schafmayer,[11] Jochen Hampe,[12] Amélie Bonnefond,[1,2] François Pattou,[3] and Philippe Froguel[1,2]

Diabetes 2018;67:1310–1321 | https://doi.org/10.2337/db17-1539

In type 2 diabetes (T2D), hepatic insulin resistance is strongly associated with nonalcoholic fatty liver disease (NAFLD). In this study, we hypothesized that the DNA methylome of livers from patients with T2D compared with livers of individuals with normal plasma glucose levels can unveil some mechanism of hepatic insulin resistance that could link to NAFLD. Using DNA methylome and transcriptome analyses of livers from obese individuals, we found that hypomethylation at a CpG site in *PDGFA* (encoding platelet-derived growth factor α) and *PDGFA* overexpression are both associated with increased T2D risk, hyperinsulinemia, increased insulin resistance, and increased steatohepatitis risk. Genetic risk score studies and human cell modeling pointed to a causative effect of high insulin levels on *PDGFA* CpG site hypomethylation, *PDGFA* overexpression, and increased PDGF-AA secretion from the liver. We found that PDGF-AA secretion further stimulates its own expression through protein kinase C activity and contributes to insulin resistance through decreased expression of insulin receptor substrate 1 and of insulin receptor. Importantly, hepatocyte insulin sensitivity can be restored by PDGF-AA–blocking antibodies, PDGF receptor inhibitors, and by metformin, opening therapeutic avenues. Therefore, in the liver of obese patients with T2D, the increased PDGF-AA signaling contributes to insulin resistance, opening new therapeutic avenues against T2D and possibly NAFLD.

In type 2 diabetes (T2D), hepatic insulin resistance is a major contributor of fasting and postprandial hyperglycemia. Although intrahepatic increased lipids and chronic elevated plasma insulin have been incriminated, the intracellular molecular mechanism that accounts for the impaired insulin signaling in livers of patients with T2D is still incompletely understood. Moreover, in T2D, hepatic

[1]University Lille, Centre National de la Recherche Scientifique, Institut Pasteur de Lille, UMR 8199 - European Genomic Institute for Diabetes, Lille, France
[2]Section of Genomics of Common Disease, Department of Medicine, Imperial College London, London, U.K.
[3]University Lille, INSERM, CHU Lille, U1190 - European Genomic Institute for Diabetes, Lille, France
[4]Department of Experimental Diabetology, German Institute of Human Nutrition Potsdam-Rehbrücke, Nuthetal, and German Center for Diabetes Research (DZD), München-Neuherberg, Germany
[5]Inserm U1016, Institut Cochin, Centre National de la Recherche Scientifique UMR 8104, Université Paris Descartes, Sorbonne Paris Cité, Paris, France
[6]Laboratory of Integrative Systems Physiology, École Polytechnique Fédérale de Lausanne, Lausanne, Switzerland
[7]INSERM U1183, University Montpellier, Institute for Regenerative Medicine and Biotherapy, CHU Montpellier, France
[8]Department of Clinical Science, Skane University Hospital Malmö, Malmö, Sweden
[9]University Lille, INSERM, CHU Lille, U995 - Lille Inflammation Research International Center, Lille, France
[10]University Lille, INSERM, CHU Lille, Institut Pasteur de Lille, U1011- European Genomic Institute for Diabetes, Lille, France
[11]Department of Visceral and Thoracic Surgery, University Hospital Schleswig-Holstein, Kiel, Germany
[12]Medical Department 1, Technische Universität Dresden, Dresden, Germany

Corresponding authors: Philippe Froguel, p.froguel@imperial.ac.uk, and Amar Abderrahmani, amar.abderrahmani@univ-lille2.fr.

Received 18 December 2017 and accepted 26 April 2018.

This article contains Supplementary Data online at http://diabetes.diabetesjournals.org/lookup/suppl/doi:10.2337/db17-1539/-/DC1.

A.A., L.Y., R.C., M.C., F.P., and P.F. contributed equally to the study.

insulin resistance is strongly associated with nonalcoholic fatty liver disease (NAFLD) (1), suggesting that the mechanisms leading to hepatic insulin resistance contribute to the development of NAFLD, and conversely. Genome-wide association studies (GWASs) and related metabolic traits have identified many loci associated with the risk of T2D (2). However, these loci only explain 15% of T2D inheritance, and GWASs have opened limited insights into the pathophysiology of T2D, including hepatic insulin resistance (2). Several DNA methylome-wide association studies have identified candidate genes possibly involved in metabolic dysfunction of the adipose tissue, skeletal muscle, and liver in obesity and T2D (3–7). Further, epigenetic analyses of livers from obese individuals with diabetes have enabled the identification of altered expression in genes involved in glucose and lipid metabolism (3). So far, the causality of such dysregulation in the development of liver insulin resistance has not been determined.

In this study, we hypothesized that analysis of the DNA methylome of livers from patients with T2D compared with livers of individuals with normal plasma glucose levels can unveil key players of hepatic insulin resistance in response to a diabetogenic environment. Our DNA methylome- and transcriptome-wide association analyses for T2D in liver samples from obese subjects identified a reduced methylation of a CpG site within the platelet-derived growth factor (PDGF) A gene (*PDGFA*), which was correlated with an increase in *PDGFA* mRNA. *PDGFA* encodes a protein forming a PDGF-AA homodimer that is known as a liver fibrosis factor when overexpressed in the liver (8). We found that the rise of liver *PDGFA* is associated not only with increased T2D risk but also with increased nonalcoholic steatohepatitis (NASH) risk, elevated fasting plasma insulin, and insulin resistance. The increased *PDGFA* expression and PDGF-AA protein levels were reproduced in human hepatocytes made insulin resistant by long-term insulin incubation and were present in the liver of insulin-resistant rodents. Furthermore, using human hepatocytes, we have demonstrated that PDGF-AA overexpression perpetuated hepatocyte insulin resistance in an autocrine feed-forward loop mechanism, providing novel insights into the mechanism possibly linking hepatic insulin resistance and NAFLD in diabetes-associated obesity.

RESEARCH DESIGN AND METHODS

Discovery Study

Liver biopsy specimens were collected by surgery of 192 obese subjects in France. Subjects included in the discovery study were participants of the ABOS (Atlas Biologique de l'Obésité Sévère) cohort (clinicaltrials.gov, NCT01129297) including 750 morbidly obese subjects whose several tissues were collected during bariatric surgery (9). All subjects were unrelated, women, older than 35 years of age, of European origin verified by principal component analysis (PCA) using single nucleotide polymorphisms (SNPs) on the Metabochip array, nonsmokers, nondrinkers, without a history of hepatitis, and without indications of liver damage in serological analysis (aspartate aminotransferase and alanine aminotransferase levels within normal reference ranges). However, we observed a significant increase in aspartate aminotransferase and alanine aminotransferase concentrations in patients with T2D compared with control subjects (Supplementary Table 1). Overall, 96 case subjects with T2D and 96 normoglycemic participants were selected. Normoglycemia and T2D were defined using the World Health Organization/International Diabetes Federation 2006 criteria (normoglycemia: fasting plasma glucose $<$6.1 mmol/L or 2-h plasma glucose $<$7.8 mmol/L; T2D: fasting plasma glucose $\geq$7 mmol/L or 2-h plasma glucose $\geq$11 mmol/L). For calculation of intermediate metabolic traits (updated HOMA model [HOMA2] for insulin resistance and β-cell function indexes), see the Supplementary Data. All procedures were approved by local ethics committees, and each participant of the ABOS cohort signed an informed consent. The main clinical characteristics are presented in Supplementary Table 1.

Replication Study

The replication study was based on in silico data of liver samples analyzed by the Infinium HumanMethylation450 BeadChip (Illumina, San Diego, CA), as previously reported (10). Clinical characteristics are reported in Supplementary Table 2. All patients provided written, informed consent. The study protocol was approved by the Ethikkommission der Medizinischen Fakultät der Universität Kiel (D425/07, A111/99) before the beginning of the study. Liver samples were obtained percutaneously from subjects undergoing liver biopsy for suspected NAFLD or intraoperatively for assessment of liver histology. Normal control samples were from samples obtained for exclusion of liver malignancy during major oncological surgery. Patients with evidence of viral hepatitis, hemochromatosis, or alcohol consumption greater than 20 g/day for women and 30 g/day for men were excluded. None of the normal control subjects underwent preoperative chemotherapy, and liver histology demonstrated absence of cirrhosis and malignancy. A percutaneous follow-up biopsy specimen was obtained in consenting bariatric patients 5–9 months after surgery. Biopsy samples were immediately frozen in liquid nitrogen, ensuring an ex vivo time of less than 40 s in all cases.

Genome-Wide Analysis of DNA Methylation

The genome-wide analysis of DNA methylation was performed using the Infinium HumanMethylation450 BeadChip, which interrogates 482,421 CpG sites and 3,091 non-CpG sites covering 21,231 genes in the Reference Sequence database (11). We used 500 ng DNA from liver tissue for bisulfate conversion using the EZ DNA Methylation kit D5001 (Zymo Research, Orange, CA) according to the manufacturer's instructions. Details of the procedure are provided in the Supplementary Data.

SNP Genotyping, Ethnic Characterization, and Genetic Risk Score

SNP genotyping was performed with Metabochip DNA arrays (custom iSelect-Illumina genotyping arrays) using

the Illumina HiScan technology and GenomeStudio software (Illumina) (12). We selected SNPs with a call rate ≥95% and with no departures from Hardy–Weinberg equilibrium ($P > 10^{-4}$). A principal component analysis (PCA) was performed in a combined data set involving the 192 patients plus 272 subjects from the publicly available HapMap project database. Genotype calls at the 106,470 SNPs present on the Metabochip were available for these 272 subjects, comprising 87 of European ancestries (HapMap CEU), 97 of Asian ancestries (HapMap CHB), and 88 of African ancestries (HapMap YRI). The first two components were sufficient to discriminate ethnic origin (Supplementary Fig. 1), and we observed that study participants clustered well with HapMap samples of European ancestries. Details of the analysis are provided in the Supplementary Data.

Statistical Analyses

Statistical analysis and quality control were performed with R 3.1.1 software. Raw data (IDAT file format) from Infinium HumanMethylation450 BeadChips were imported into R using the *minfi* package (version 1.12.0 on Bioconductor) (13). We then applied the preprocessing method from GenomeStudio software (Illumina) using the reverse-engineered function provided in the *minfi* package. Samples were excluded when less than 75% of the markers had detection *P* values $<10^{-16}$. Markers were ruled out when less than 95% of the samples had detection *P* values $<10^{-16}$. According to this strategy, no sample was excluded, and 70,314 of 485,512 markers were excluded. For correction for Infinium HumanMethylation450 BeadChip design, which includes two probe types (type I and type II), a Beta-MIxture Quantile (BMIQ) normalization was performed (14). We also checked for outliers using PCA (*flashpcaR* package, version 1.6-2 on the Comprehensive R Archive Network).

At this stage, 416,693 markers and 192 samples were kept for further analysis. We tested the association between methylation level and diabetes status by applying a linear regression adjusted for age, BMI, steatosis (in percentage), presence of NASH, and fibrosis. Results were corrected for multiple testing using a Bonferroni correction ($P < 10^{-7}$). The association between DNA methylation and metabolic traits was analyzed using a linear regression model, including normoglycemic samples adjusted for age and BMI. Quality control was performed on the HumanHT-12 v4.0 Whole-Genome DASL HT Assay (Illumina) data, according to the following criterion: probes were kept for further analysis when the detection *P* values provided by GenomeStudio software version 3.0 (Illumina) were below 5% for all samples. A PCA was performed to identify samples with extreme transcriptomic profiles.

After the quality control just described, 18,412 probes matching 13,664 genes and 187 samples were kept and analyzed for differential expression between case subjects with T2D and control subjects, using linear regression. Methylation and expression data were tested for correlation. Linear regression analysis was used for testing the association in *cis* genes within the 500 kb with the CpG methylation site with the T2D status as a covariate. To account for multiple testing, we used 5% as a threshold for the false discovery rate.

We selected a subgroup of 24 samples among the 192 initial samples, including 12 normoglycemic and 12 case subjects with T2D, to analyze DNA methylation in blood samples from the same donors. The 24 samples were selected based on their expression and methylation profiles using PCA to reduce the heterogeneity.

Cell Culture

Immortalized human hepatocytes (IHHs) were obtained from primary human hepatocytes that were transfected with a plasmid carrying the large T antigen SV40 (15). The cells retained features of normal hepatocytes, including albumin secretion, the multidrug resistance P-glycoprotein, active uptake of the bile salt taurocholate, triglyceride-rich lipoproteins, apolipoprotein B (0.6 mg/mL per day), and apolipoprotein A-I secretion (15). IHH cells (maintained at passages 35–45) were cultured in Williams E medium (Invitrogen), containing 11 mmol/L glucose and supplemented with 10% FCS (Eurobio), 100 units/mL penicillin, 100 μg/mL streptomycin, 20 mU/mL insulin (Sigma-Aldrich), and 50 nmol/L dexamethasone (Sigma-Aldrich) (16). For insulin pretreatment, 10^6 cells were cultured in six-well plates in DMEM (Invitrogen) with or without 100 nmol/L human insulin (Novo Nordisk) supplemented with 5 mmol/L glucose, 2% FCS, 100 units/mL penicillin, and 100 μg/mL streptomycin for 24 h. For monitoring insulin signaling, medium was removed and replaced by FCS- and phenol red–free DMEM medium, with or without 200 nmol/L human insulin, for 1 h. Human hepatocytes were isolated from liver lobectomies resected for medical reasons as described (17) in agreement with the ethics procedures and adequate authorization.

RNA sequencing, microarray mRNA expression analysis, quantitative (q)RT-PCR, Western blotting, chemicals, ELISA, glycogen measurement, global serine/threonine kinases activity, DNA/RNA preparation, Oil Red O staining, cell proliferation, apoptosis, and intermediate metabolic traits. See the Supplementary Experimental Procedure in the Supplementary Data.

RESULTS

Liver Epigenetic Modification in T2D

The liver DNA methylome was assessed in 96 age- and BMI-matched obese women with T2D and 96 obese women with normal glucose levels (Supplementary Table 1). Although we initially identified 381 differentially methylated regions (DMRs) in the liver from obese patients with T2D compared with obese patients with normal glucose (Supplementary Fig. 2), we only observed one genome-wide significant DMR (cg14496282 within *PDGFA*) in obese patients with T2D after adjusting for liver steatosis and NASH, in an attempt to control for confounding effects (Supplementary Table 1). The methylation at cg14496282 was associated with decreased T2D risk ($\beta = -15.6\%$; $P = 2.5 \times 10^{-8}$)

(Fig. 1*A* and *B*). The average DNA methylation at cg14496282 was 41.3% in patients with T2D and 60.3% in control subjects, which corresponds to a 1.46-fold decrease in the methylation level of the CpG site. We used mathematical deconvolution analysis (18) to check the methylation at this CpG site for possible confounding effects due to differences in cell composition, and we still observed consistent effects for T2D risk ($\beta = -14.9\%$; $P = 6.9 \times 10^{-7}$). We replicated this association in the liver from 12 case subjects with T2D and 53 German control subjects (10) and found that T2D risk was associated with decreased methylation level at the cg14496282 site ($\beta = -14.0\%$; $P = 0.01$) (Supplementary Table 2). A decreased methylation level in another CpG site within *PDGFA* has been found in the liver from obese men with T2D compared with nonobese control subjects from another cohort (3), supporting that *PDGFA* is a target for epigenetic modification in response to obesity-associated diabetes.

We next investigated whether the T2D-associated *PDGFA* cg14496282 hypomethylation was specific to the liver. We assessed the blood DNA methylome from 12 obese case subjects with T2D and 12 obese control subjects with normal glucose presenting with extreme liver methylation levels at cg14496282. We found a significant correlation between methylation levels in blood and liver ($r = 0.66$; $P = 6.61 \times 10^{-4}$) and a slightly reduced methylation at the cg14496282 site ($\beta = -1.4\%$; $P = 0.01$) in the blood of subjects with T2D compared with control subjects. We also compared DNA methylation at cg14496282 in 43 liver and skeletal muscle samples from 192 participants who were randomly selected from the ABOS cohort, but we did not find any significant correlation ($P > 0.05$).

In the 192 obese liver samples, we next investigated *cis*-located genes (within 500 kb around cg14496282) that were differentially expressed between case subjects with T2D and control subjects and which mRNA expression correlated with DNA methylation at the *PDGFA* cg14496282 site. Using a false discovery rate threshold of 5% for differential expression analysis and methylation-expression correlation analysis, we identified that the methylation at cg14496282 is negatively associated with the expression of *PDGFA* in case subjects with T2D and control subjects with normal glucose ($P < 0.007$) (Table 1).

Reduced Liver *PDGFA* Expression Is Associated With Lower Hepatic Fibrosis Risk

In subjects with T2D and in normoglycemic control subjects, we found that *PDGFA* cg14496282 methylation was significantly associated with decreased NASH risk ($P < 0.05$) (Table 1), whereas *PDGFA* expression in the liver

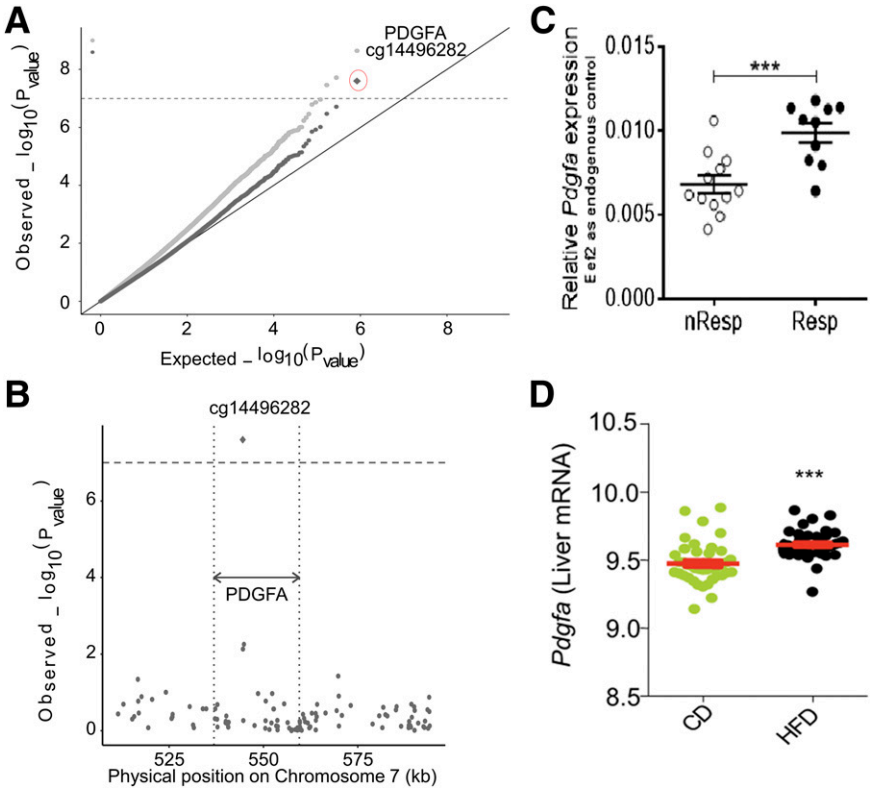

Figure 1—*A*: Quantile-quantile plot shows the residual inflation of test statistics before and after genomic-control correction. *B*: Manhattan plot centered on *PDGFA* cg14496282 methylation site shows the association signal within *PDGFA* bounds. *C* and *D*: Hepatic *Pdgfa* expression in 6-week-old male B6 mice that were diet-induced obese (DIO) responder (Resp, $n = 12$) and DIO nonresponder (nResp, $n = 10$) (*C*) and in BXD mice ($n = 45$) fed a chow diet (CD) or a high-fat diet (HFD) for 21 weeks (*D*). ***$P < 0.0001$ by unpaired *t* test with Welch correction.

Table 1—Association of liver methylation levels of cg14496282 and liver *PDGFA* gene expression with multiple quantitative and binary traits

	PDGFA cg14496282 methylation		*PDGFA* expression	
	Effect size in % of methylation/trait unit (*P* value)		Effect size in SD/trait unit (*P* value)	
Traits (unit)	Control subjects	Case subjects with T2D	Control subjects	Case subjects with T2D
cg14496282 methylation (%)			**-1.44 (6.27×10^{-3})**	**-2.497 (4.94×10^{-3})**
PDGFA expression (scaled SD)	**-0.0548 (6.27×10^{-3})**	**-0.0338 (4.94×10^{-3})**		
Fasting glucose (mmol/L)	-0.0112 (0.79)		0.292 (0.196)	
Fasting insulin (pmol/L)	**-1.45×10^{-3} (2.32×10^{-3})**		**6.83×10^{-3} (9.49×10^{-3})**	
HOMA2-β (unitless - log)	**-0.169 (2.92×10^{-3})**		**0.626 (0.038)**	
HOMA2-IR (unitless - log)	**-0.104 (4.93×10^{-3})**		**0.528 (7.47×10^{-3})**	
QUICKI (unitless)	**1.66 (0.01)**		**-9.192 (9.78×10^{-3})**	
Steatosis (%)	**-2.15×10^{-3} (0.01)**	-4.34×10^{-4} (0.42)	**0.0136 (2.72×10^{-3})**	**0.020 (2.14×10^{-6})**
NASH (yes/no)	**-0.17 (0.04)**	**-0.072 (0.03)**	**2.115 (9.38×10^{-7})**	**1.447 (3.37×10^{-8})**
Hepatic fibrosis (yes/no)	-0.07 (0.09)	**-0.051 (0.04)**	0.187 (0.434)	**0.631 (2.66×10^{-3})**
Aminotransferase				
Alanine (IU/L)	-1.44×10^{-4} (0.89)	**-1.34×10^{-3} (0.03)**	0.0106 (0.067)	**0.0194 (1.46×10^{-4})**
Aspartate (IU/L)	-4.72×10^{-3} (0.06)	**-1.76×10^{-3} (0.04)**	**0.0342 (7.89×10^{-3})**	**0.0327 (2.56×10^{-6})**

HOMA2-β, updated HOMA model of β-cell function; HOMA2-IR, updated HOMA model of insulin resistance; QUICKI, quantitative insulin-sensitivity check index. Methylation levels at cg14496282 and *PDGFA* gene expression are the endogenous variable in all linear regressions used to measure associations. Bold values are statistically significant.

was associated with increased NASH risk ($P < 0.01$) (Table 1). Furthermore, in patients with T2D, *PDGFA* cg14496282 methylation was significantly associated with decreased hepatic fibrosis, decreased alanine aminotransferase levels, and decreased aspartate aminotransferase levels ($P < 0.05$) (Table 1), whereas *PDGFA* expression in the liver was associated with increased hepatic fibrosis and increased liver enzyme levels ($P < 0.01$) (Table 1). These results were in line with previous studies that showed that *PDGFA* cg14496282 hypomethylation is associated with increased *PDGFA* liver expression in advanced versus mild human NAFLD (19,20). *PDGFA* encodes a dimer disulfide-linked polypeptide (PDGF-AA) that plays a crucial role in organogenesis and cirrhotic liver regeneration (21, 22). Overexpression of PDGF-AA in mouse liver causes spontaneous liver fibrosis (8). Moreover, activation of PDGF receptor signaling stimulates hepatic stellate cells and thereby promotes liver fibrosis (23–25).

Increased Liver *PDGFA* Expression Is Associated With Hyperinsulinemia and Insulin Resistance

In obese subjects with normal glucose levels, we next found that *PDGFA* cg14496282 methylation is significantly associated with decreased fasting serum insulin levels and decreased insulin resistance as modeled by the HOMA index HOMA2-insulin resistance ($\beta = -1.45 \times 10^{-3}$, $P = 2.32 \times 10^{-3}$; and $\beta = -0.10$, $P = 4.93 \times 10^{-3}$, respectively) (Table 1). In contrast, *PDGFA* liver expression was significantly associated with increased fasting serum insulin levels and increased insulin resistance ($\beta = 6.83 \times 10^{-3}$, $P = 9.49 \times 10^{-3}$; and $\beta = 0.53$, $P = 7.47 \times 10^{-3}$, respectively) (Table 1).

We next calculated a genetic risk score (GRS) as the sum of alleles increasing fasting insulin levels over 19 GWAS-identified SNPs (26) and found that this GRS is associated with decreased DNA methylation at cg14496282 ($\beta = -1.05\%$ per allele; $P = 4 \times 10^{-3}$) (Supplementary Table 3). This association remained significant when we analyzed case subjects with T2D and control subjects separately (and then meta-analyzed) or when we adjusted for BMI, HDL cholesterol, or triglycerides; these traits having a genetic overlap with fasting insulin (26). These results strongly suggested that hyperinsulinemia (and associated insulin resistance) contributes to decreased DNA methylation of *PDGFA* cg14496282 and, consequently, to the increase in the *PDGFA* expression. In contrast, the GRS including 24 SNPs associated with fasting glucose, the GRS including 65 SNPs associated with T2D, and the GRS including 97 SNPs associated with BMI, were not associated with cg14496282 methylation (Supplementary Table 3). These results suggest that hyperglycemia and obesity per se are not involved in the modulation of *PDGFA* methylation and expression.

The in vivo association between liver *PDGFA* overexpression and insulin resistance was supported by the data obtained from different mice models of insulin resistance associated with obesity. In the liver from C57BL/6J (B6) mice that are susceptible to diet-induced obesity (27), we found that *Pdgfa* expression is increased by 46% compared with control mice (i.e., that do not respond to a high-fat diet) (Fig. 1*C*). Similarly, we found that liver *Pdgfa* expression is increased in insulin-resistant BXD mice fed a high-fat

diet for 21 weeks compared with control mice (Fig. 1*D*). However, the cg14496282 CpG site is not conserved in mice (28), suggesting that different epigenetic mechanisms rely on the rise of *Pdgfa/PDGFA* in insulin-resistant hepatocytes in mice and humans.

Increased *PDGFA* Expression and Secretion From Insulin-Resistant Human Hepatocytes

The association of increased liver *PDGFA* expression with systemic insulin resistance in obese subjects suggests that *PDGFA* overexpression plays a role in liver insulin resistance and thereby in T2D development. Chronic hyperinsulinemia indeed induces liver insulin resistance (29), and *PDGFA* has an autocrine function on hepatocytes (21). In this context, the exposure of mouse embryo cells to PDGF-AA inhibits insulin signaling (30). We therefore hypothesized that the obesity-associated increased *PDGFA* expression contributes to mediate the deleterious effects of chronic hyperinsulinemia on hepatic insulin resistance. To assess this hypothesis, we established an in vitro model of insulin-resistant human hepatocytes caused by hyperinsulinemia. To do so, we used the IHHs. IHH cells are indeed equipped with the functional machinery for glucose metabolism (16) and secrete PDGF-AA homodimer at comparable levels with primary human hepatocytes (Fig. 2*A*). Exposure of IHH cells to insulin for 16 or 24 h hampered insulin-induced phosphorylation of AKT serine/threonine kinase at residue serine 473 (Fig. 2*B*). In line with the pivotal role of AKT activation in glycogen synthesis (31), we found reduced insulin-induced glycogen production in IHH cells exposed to insulin for 16 h and 24 h (Fig. 2*C*). The defective insulin signaling by insulin was accompanied by a rise in *PDGFA* mRNA and in abundance and secretion of the encoded protein PDGF-AA homodimer from IHH cells (Fig. 2*D–F*). In addition, the insulin-induced increase in *PDGFA* expression was associated with the reduced cg14496282 CpG methylation level in IHH cells (Fig. 2*G*), suggesting that insulin resistance induced by hyperinsulinemia accounts for the rise of *PDGFA* in hepatocytes of obese individuals with diabetes. Because these results may be cell-line dependent, we measured AKT phosphorylation in liver hepatocellular HepG2 cells exposed to insulin for 24 h and retrieved similar results (Fig. 2*H*). In HepG2 cells, the expression of *PDGFA* was also significantly increased after long-term insulin incubation (Fig. 2*I*). On one hand, the increase in *PDGFA* mRNA seemed specific to insulin exposure because insulin treatment did not modify cell proliferation (Supplementary Fig. 3) or intracellular neutral lipid levels (Supplementary Fig. 4). On the other hand, palmitate exposure did not change *PDGFA* expression in IHH cells (Supplementary Fig. 4).

PDGF-AA Contributes to Insulin Resistance Induced by Insulin

Our data suggest that PDGF-AA secretion in the liver of obese individuals with T2D is induced by hyperinsulinemia and not the excess of fatty acids influx. We then hypothesized that PDGF-AA directly causes insulin resistance in human hepatocytes. In line with this hypothesis, we found that the culture of IHH cells with a human PDGF-AA recombinant inhibits insulin-induced AKT activation (Fig. 3*A*). In contrast, the incubation of IHH cells with anti–PDGF-AA–blocking antibodies reversed the deleterious effect of long-term insulin exposure on AKT phosphorylation (Fig. 3*B*). We then investigated the mechanism whereby PDGF-AA inhibits AKT activation. Human hepatocytes express PDGF receptors (PDGFR), including PDGFRα and PDGFRβ, which both bind PDGF-AA (8). We used the PDGFR inhibitor Ki11502 to test the role of PDGFR signaling (32). Pretreatment of IHH cells with Ki11502 efficiently antagonized the negative effect of insulin on AKT phosphorylation, mimicking results obtained with antibodies blocking PDGF-AA (Fig. 3*C*). PDGFR blockade by Ki11502 increased the ability of insulin to stimulate glycogen synthesis (Fig. 3*D*).

To further dissect the signaling pathways by which both insulin and PDGF-AA impair AKT and insulin action, we performed a global measurement of serine/threonine protein kinases (STKs) using STK PamGene arrays consisting of 140 immobilized serine/threonine-containing peptides that are targets of most known kinases (33). We looked for differential STK activity between control and IHH cells cultured with insulin for 24 h. Peptides with phosphorylation that varied significantly between the two conditions were indicative of differential specific STK activities. This unbiased kinase analyses underscored significant differences in activities of protein kinase C (PKC) Θ and PKCε (Fig. 4*A*). The activation of these two PKCs hampers insulin signaling in response to chronic hyperlipidemia (34–36). These two kinases are also known to phosphorylate the insulin receptor substrate 1 (IRS1) and the insulin receptor (INSR) on serine residues, which impairs the association of INSR with IRS proteins and leads to the blockade of AKT activation and of the downstream signaling pathways (35,36). We therefore treated IHH cells with phorbol 12-myristate 13-actetate (PMA), a potent activator of PKCs, and retrieved AKT inhibition (Supplementary Fig. 5). PKCΘ and PKCε activities are linked to their phosphorylation at serine 676 and serine 729, respectively (37,38). In IHH cells cultured with insulin for 16 h or 24 h, we found a striking phosphorylation of the two PKCs, which coincided with the decreased AKT phosphorylation (Fig. 4*B*). The effect of insulin on the phosphorylation of the two kinases is likely to rely on PDGF-AA, because the PKCΘ and PKCε were directly activated by PDGF-AA (Fig. 4*C*). Activation of PKCε decreases INSR abundance (34). In line with this result, we found in IHH cells cultured with insulin and PDGF-AA that an impaired INSR content is closely linked to reduced INSR tyrosine phosphorylation at residue Y972 (Fig. 4*D*). In addition, the PKCε-mediated T1376 phosphorylation, which inactivates the INSR, was increased in response to insulin or PDGF-AA (Fig. 4*E*).

To gain further insights into the intracellular mechanism through which PDGF-AA alters insulin signaling

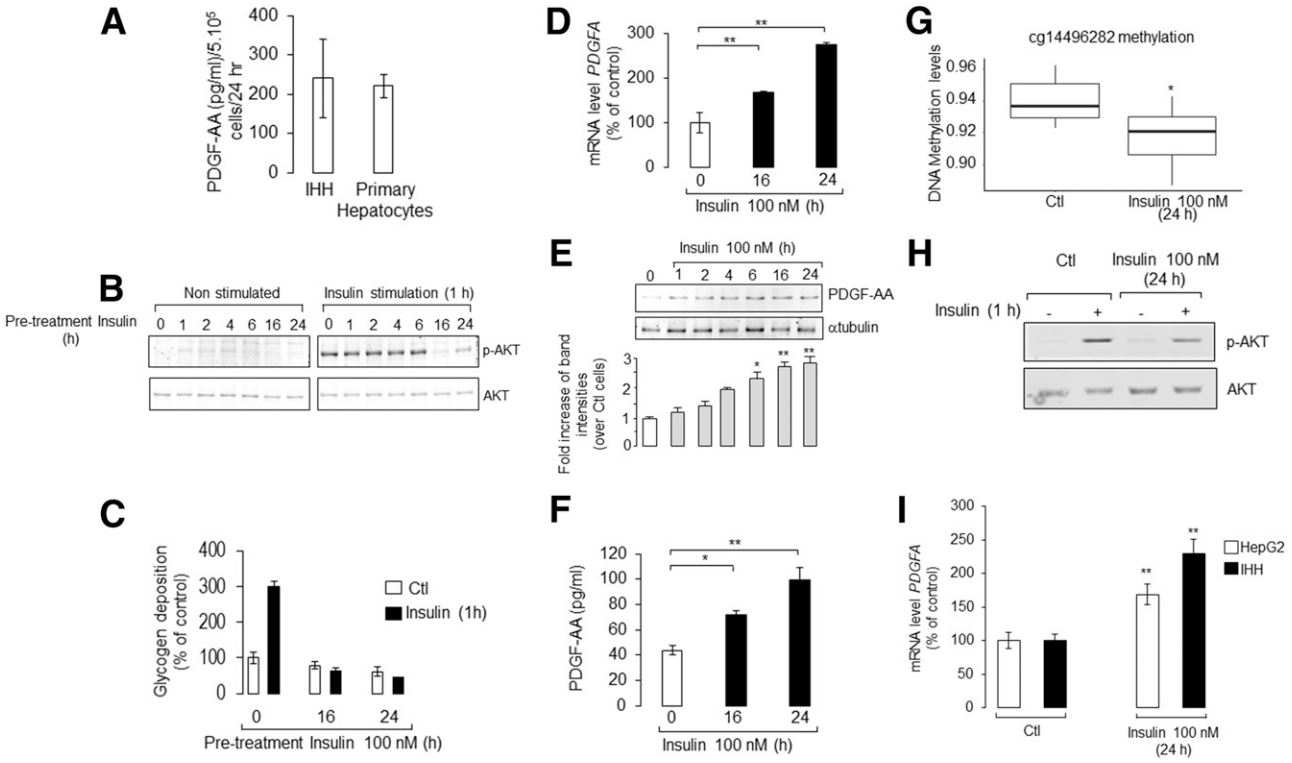

Figure 2—*A*: PDGF-AA secretion from IHH cells and primary human hepatocytes was measured by ELISA kit. *B*: Measurement of insulin-induced AKT phosphorylation (p-AKT) in response to human insulin (Novo Nordisk) for the indicated times. IHH cells were incubated for the indicated times in a culture medium containing 5 mmol/L glucose and 2% FCS, with or without 100 nmol/L human insulin. AKT phosphorylation was stimulated by 200 nmol/L insulin for 1 h. Immunoblotting for p-AKT was done using the anti–p-AKT (serine 473) antibodies. Results of a representative experiment of three are shown. *C*: Effect of insulin on the glycogen production. Insulin-induced glycogen production was measured by ELISA in IHH cells that were precultured with 100 nmol/L insulin for 16 h and 24 h. Ctl, control. *D*: Increase of *PDGFA* mRNA by insulin. IHH cells were cultured with 100 nmol/L human insulin for 16 h and 24 h. The *PDGFA* mRNA level was quantified by qRT-PCR and normalized against *RPLP0*. The expression levels from untreated cells were set to 100%. Data are the mean ± SEM. *E*: PDGF-AA abundance in IHH cells cultured with insulin. IHH cells were cultured with 100 nmol/L human insulin for the indicated times. PDGF-AA content was quantified by Western blotting. The blot is one representative of three independent experiments. *F*: PDGF-AA secretion in response to insulin. IHH cells were cultured with insulin for the indicated times. ELISA was used to measure PDGF-AA from the supernatant that was retrieved from the cultured IHH cells. *G*: Methylation levels at *PDGFA* cg14496282 in response to insulin. IHH cells were cultured in a culture medium for 24 h containing 5 mmol/L glucose and 2% FCS, with or without 100 nmol/L human insulin. The methylation level at cg14496282 was quantified by the Infinium HumanMethylation450 BeadChip. *H*: Effect of chronic insulin in insulin-induced AKT activation in HepG2 cells. HepG2 cells were incubated for 24 h in a culture medium with 100 nmol/L human insulin or without (Ctl). AKT phosphorylation was stimulated by 200 nmol/L insulin for 1 h. Immunoblotting for phosphorylated-AKT (p-AKT) was done using anti–p-AKT (serine 473) antibodies. The result of a representative experiment of three is shown. *I*: Increase of *PDGFA* mRNA by insulin in HepG2 cells. The *PDGFA* mRNA level was quantified by qRT-PCR in HepG2 and IHH cells that were cultured with insulin for 24 h. The *PDGFA* mRNA was normalized against *RPLP0*. The expression levels from untreated cells were set to 100%. Data are the mean ± SEM. $^*P < 0.05$; $^{**}P < 0.001$.

in hepatocytes, we performed RNA sequencing of IHH cells treated or not with insulin for 24 h. We found a profound dysregulation of expression of genes involved in carbohydrate metabolism, inflammatory, and insulin-signaling pathways in response to insulin. Indeed, when we grew a network based on *PDGFA* through Ingenuity Pathway Analysis (IPA), we found a significant increase in the expression of genes of the vascular endothelial growth factor and PDGF families, including as expected *PDGFA* ($\log_2$ fold change = 0.80; $P = 1.1 \times 10^{-11}$) (Supplementary Fig. 6 and Supplementary Table 5). Subsequently, we analyzed the diseases and/or functions highlighted by the insulin-evoked deregulated expressed genes in IHH cells. Among the significant outputs, we found a network related to the metabolism of carbohydrates that includes *PDGFA* ($P = 1.2 \times 10^{-6}$) (Supplementary Fig. 7 and Supplementary Table 5). We also identified in IHH cells cultured with insulin for 24 h a decrease in the expression of the *IRS1* gene (Fig. 5*A*, Supplementary Fig. 6, and Supplementary Table 6). The decreased *IRS1* expression by insulin was confirmed by Western blotting (Fig. 5*B*) and mimicked by PDGF-AA (Fig. 5*C*). Silencing of *IRS1* expression using small interfering (si)RNAs confirmed that the IRS1 abundance is critical for AKT activation in IHH cells in response to insulin (Fig. 5*D*). A defective IRS1 level can therefore account for the impaired insulin signaling caused by PDGF-AA in insulin-resistant hepatocytes. The decrease of *IRS1* mRNA and protein level is mediated by PKC activity since its inhibition by sotrastaurin, a PKCΘ and PKCε inhibitor (39), prevented the reduction of IRS1 caused by hyperinsulinemia (Fig. 5*E* and *F*), and in

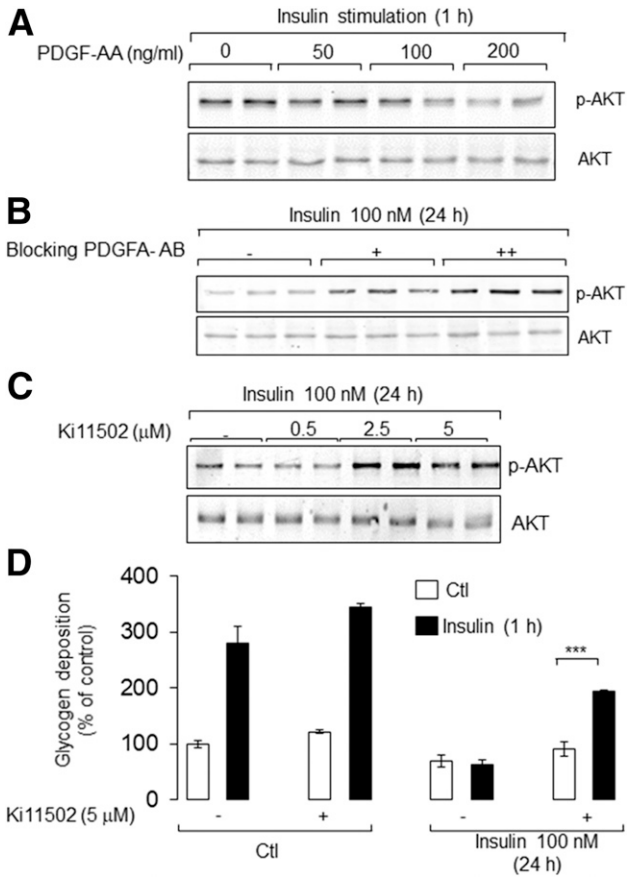

Figure 3—Effects of human PDGF-AA recombinant (*A*), *PDGFA* blocking antibodies (*B*), or the PDGFR inhibitor ki11502 (*C*) on insulin-induced AKT activation. Activation of AKT was monitored by Western blotting using total proteins from IHH cells that were cultured with the human recombinant PDGF-AA at the indicated concentrations for 24 h, which subsequently were incubated with 200 nmol/L insulin for stimulating phosphorylation of AKT (p-AKT). IHH cells were co-incubated in a culture medium containing 5 mmol/L glucose and 2% FCS, with or without 100 nmol/L human insulin, for 24 h plus PDGF-AA at the indicated concentration (*A*), *PDGFA* antibodies (+, 0.75 μg; ++, 1.5 μg) (*B*), or ki11502 (*C*) at the indicated concentration. The result of a representative experiment of three is shown. *D*: Effect of the PDGFR inhibitor ki11502 on glycogen production. Glycogen was measured by ELISA in IHH cells that were cocultured with 5 μmol/L ki11502 and insulin for the indicated times. Glycogen was monitored after stimulating cells in a Krebs-Ringer phosphate buffer without (control [Ctl]) or with insulin for 1 h and 20 mmol/L glucose. Glycogen was monitored by ELISA. ***$P < 0.001$.

contrast, PKC activation by PMA mimicked the effect of insulin (Fig. 5*G* and *H*).

Altogether, our data suggest a role for hepatocyte PDGF-AA in promoting further liver insulin resistance via the decrease of INSR and IRS1 and the activation of both PKCΘ and PKCε.

Autocrine Regulation of PDGF-AA on Its Expression and the Beneficial Effects of Metformin

PDGF-AA stimulates its own expression in the liver (40). This suggests that in insulin-resistant hepatocytes, PDGF-AA amplifies its secretion, thereby perpetuating insulin resistance. We found that culture of IHH cells with PDGF-AA stimulated *PDGFA* expression (Fig. 6*A*) and PDGF-AA secretion (Supplementary Fig. 6). The effect of PDGF-AA on its expression was mediated by PDGFR because the PDGFR tyrosine kinase inhibitor ki11502 prevented the rise of *PDGFA* mRNA of cells exposed to insulin or to human PDGF-AA (Fig. 6*A* and *B*). The overexpression of *PDGFA* by PDGF-AA may require PKC activation because the PMA mimicked both insulin and PDGF-AA effects on the *PDGFA* mRNA (Fig. 6*D*), and inversely, the inhibitor sotrastaurin, alleviated the rise of *PDGFA* (Fig. 6*E*). Altogether, hyperinsulinemia-induced PDGF-AA likely aggravates its overexpression in T2D and its consequences (Fig. 7). Metformin, the most prescribed T2D drug, inhibits PKCε (41) and has been specifically proposed for patients with diabetes with NAFLD and hepatocarcinoma (HCC) (42). Furthermore, metformin reduces HCC incidence in patients with diabetes in a dose-dependent manner (43). We found that metformin also efficiently abolished the expression of insulin-induced *PDGFA* mRNA (Supplementary Fig. 8*A*), protein content (Supplementary Fig. 8*B*), and secretion (Supplementary Fig. 8*C*). Thus, a part of the effects of metformin on insulin sensitivity may be mediated by the reduction of *PDGFA* overexpression in hepatocytes.

DISCUSSION

GWAS have only identified so far few genes involved in NAFLD (44), and the contribution of epigenetics to T2D liver dysfunction is still elusive. Although we initially identified 381 DMRs in the liver from obese patients with T2D compared with normal glucose obese patients, we only observed one genome-wide significant DMR (cg14496282 within *PDGFA*), associated with the increase of *PDGFA* expression in *cis*, in obese patients with T2D after adjusting for possible confounding effects of liver steatosis and NASH. The cg14496282 might be instrumental in the functional impairment of the liver in obesity-associated T2D. Notably, we found that liver *PDGFA* cg14496282 hypomethylation and concomitant rise in liver *PDGFA* expression were also associated with systemic insulin resistance in obese patients without diabetes but not with their glucose values. Elevated *PDGFA* expression was also reported in biliary atresia (45) and is a diagnostic and prognostic biomarker of cholangiocarcinoma, a liver cancer associated with severe insulin resistance (but paradoxically not with obesity) (32,46). Thus, *PDGFA* seems to be a liver marker of insulin resistance and of chronic hyperinsulinemia. Furthermore, the genetic data from our analysis of GRS related to insulin resistance suggest a causative effect of plasma insulin levels on the methylation level, hepatic expression, and secretion of this growth factor. The elevated *PDGFA* expression in human liver from obese subjects can therefore be directly due to their severe hyperinsulinemia.

PDGFA encodes a dimer disulfide-linked polypeptide (PDGF-AA) that plays a crucial role in organogenesis (21). The activation of PDGF-AA receptor signaling is involved

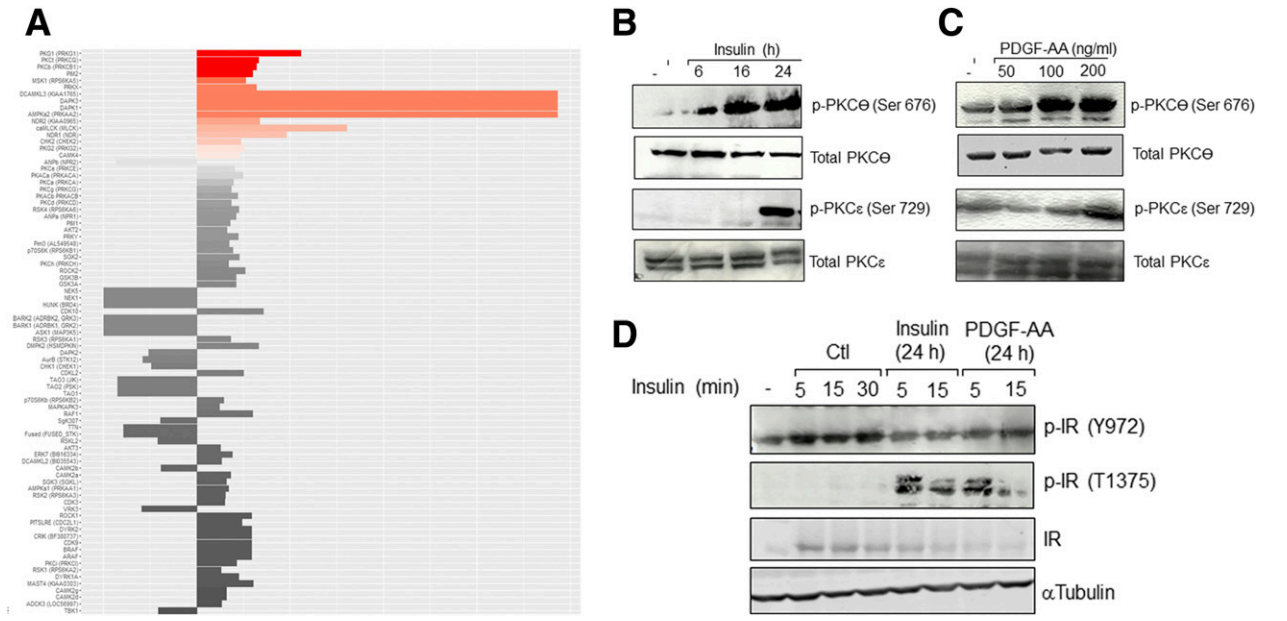

Figure 4—*A*: Volcano plot shows differences in putative serine/threonine kinase activities between control and insulin-treated IHH cells for 24 h. Specific and positive kinase statistics (in red) show higher activity in IHHs cultured with insulin compared with control samples. Effects of insulin (*B*) and PDGF-AA (*C*) on the phosphorylation (p-) of PKCΘ and PKCε. IHH cells were cultured with insulin for the indicated times or PDGF-AA (for 24 h). p-PKCΘ (Ser 676) and p-PKCε (Ser 729) were measured by Western blotting and normalized against total PKCΘ and PKCε. *D*: Effect of insulin and PDGF-AA on the tyrosine phosphorylation of INSR (p-IR [Y972]), threonine phosphorylation of INSR (p-IR [T1376]), INSR abundance (IR), and α-tubulin. Western blotting experiments were achieved from total proteins of IHH cells cultured with 100 nmol/L insulin or 100 ng/mL PDGF-AA for 24 h. p-INSR was done by stimulating IHH cells with insulin for 1 h. The result of a representative experiment of three is shown. Ctl, control.

in cirrhotic liver regeneration (22), and the chronic elevation of PDGF-AA in mouse liver induces fibrosis (8). High PDGF-AA levels contribute to hepatic fibrogenesis by activating hepatic stellate cells in mice (23–25). The association of increased *PDGFA* expression with liver steatosis and fibrosis observed in our study and in others supports a similar fibrogenic role in the human liver (19,20), in which chronic hyperinsulinemia might be instrumental (47). Thus, the PDGF-AA secreted by

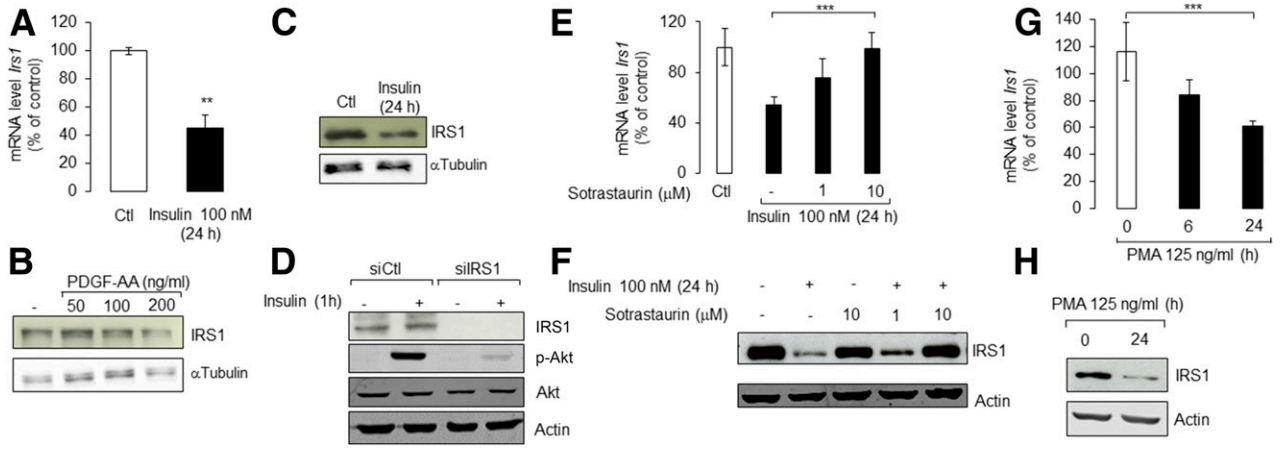

Figure 5—Effect of insulin on *IRS1* mRNA level (*A*) and protein (*B*). The *IRS1* mRNA level and IRS1 abundance was quantified by qRT-PCR and Western blotting in IHH cells cultured with 100 nmol/L insulin for 24 h. The *IRS1* mRNA was normalized against *RPLP0*. The expression levels from untreated control (Ctl) cells were set to 100%. Data are the mean ± SEM. $^{**}P < 0.001$. *C*: Effect of PDGF-AA on the IRS1 content. IHH cells were cultured with PDGF-AA at the indicated concentrations for 24 h. Results of a representative experiment of three are shown. *D*: Effect of siRNAs against IRS1 on insulin-induced AKT activation. Duplexes of siRNAs were transfected in IHH cells for 48 h. Thereafter, phosphorylation of AKT (p-AKT) on the serine 473 was induced with insulin for 1 h. Results a representative experiment of three are shown. Effect of the PKC inhibitor sotrastaurin PKC (*E* and *F*) and PMA PKC activator (*G* and *H*) on the expression of *IRS1* mRNA and protein. *PDGFA* mRNA was quantified in IHH cells cultured with sotrastaurin at the indicated concentration in the presence of 100 nmol/L insulin for 24 h or PMA for the indicated times. The *IRS1* mRNA was normalized against *RPLP0*. The expression levels from untreated cells were set to 100%. Data are the mean ± SEM of three independent experiments made in triplicates. $^{***}P < 0.0001$.

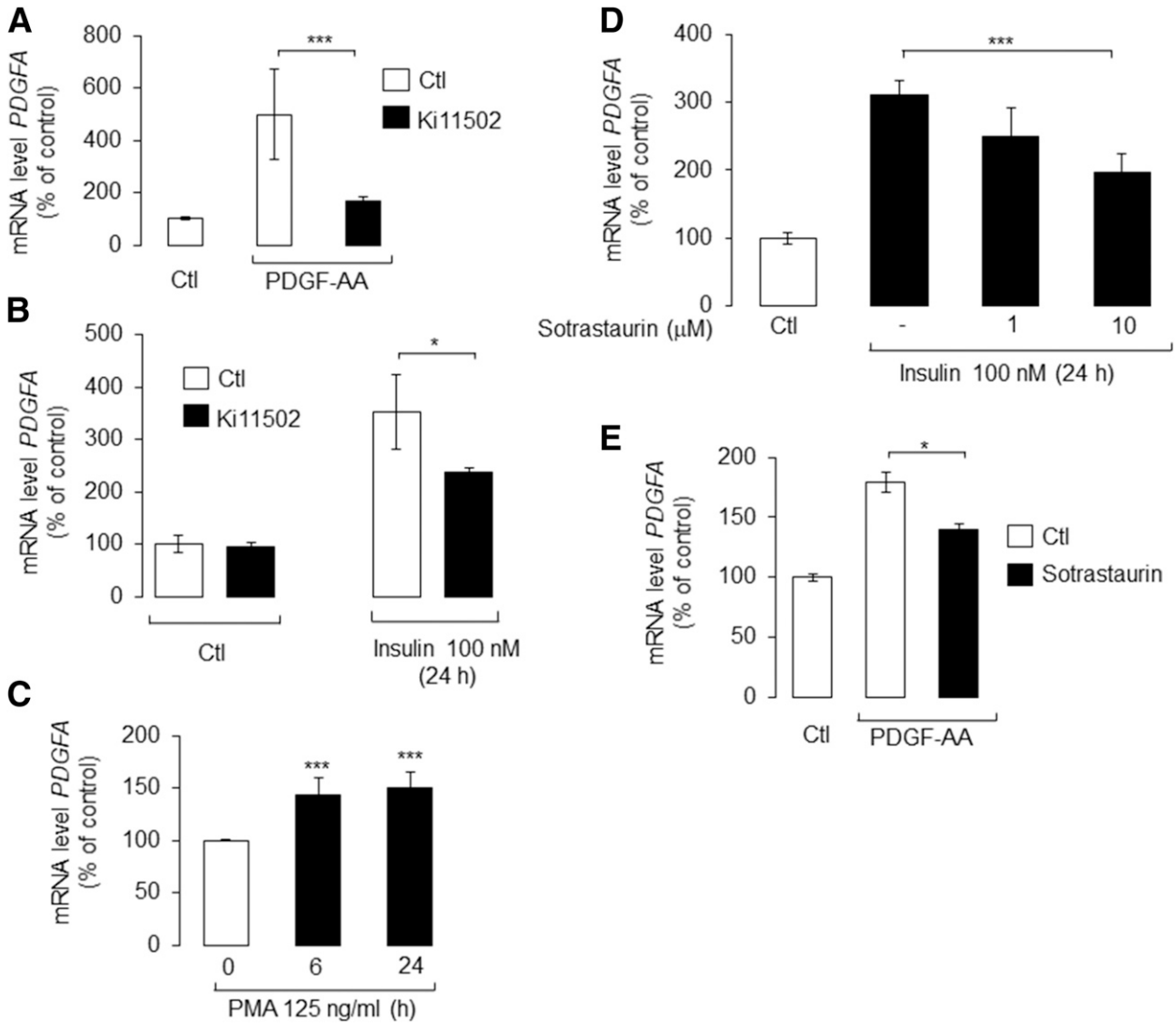

Figure 6—Effect of ki11502 PDGFR inhibitor on the *PDGFA* expression in response to PDGF-AA (*A*) and insulin (*B*). Ctl, control. IHH cells were cultured for 24 h with 100 ng/mL PDGF-AA or 100 nmol/L insulin in the presence or absence of 5 μmol/L ki11502 for 24 h. Effect of PKC activator PMA (*C*) and the PKC inhibitor sotrastaurin (*D* and *E*) on the expression of *PDGFA* mRNA induced by insulin (*D*) or PDGF-AA (*E*). *PDGFA* mRNA was quantified by qRT-PCR in IHH cells cultured with PMA for the indicated times, 100 nmol/L insulin, or 100 ng/mL PDGF-AA in the presence of 1 μmol/L sotrastaurin or at the indicated concentration for 24 h. *PDGFA* mRNA was normalized against *RPLP0*. The expression levels from untreated cells were set to 100%. Data are the mean ± SEM of three independent experiments made in triplicates. $^*P < 0.05$; $^{***}P < 0.0001$.

the liver in response to chronic hyperinsulinemia possibly contributes, alone and/or in combination with any of the 380 epigenetically modified genes, to liver steatosis and fibrogenesis in obese people with diabetes.

We also believe that PDGF-AA may contribute to the inhibitory effect of chronic hyperinsulinemia on hepatocyte insulin signaling via a feedback autocrine loop (Fig. 6*F*). PDGF-AA stimulates its own expression via the activation of PKC. This vicious cycle perpetuates a high PDGF-AA level and thereby continuous insulin resistance. Further studies will determine whether hyperinsulinemia per se and/or accumulation of secreted PDGF-AA initiate the induction of *PDGFA*. Our data further suggested that the negative effect of PDGF-AA on insulin signaling is the consequence of the decrease of IRS1 and INSR, and PKC activation, including PKCΘ and PKCε. These two kinases are known to phosphorylate IRS-1 and the insulin receptor on serine residues, which impairs the association of the insulin receptor with IRS proteins and leads to the blockade of AKT activation and of the downstream signaling (35,36).

Our findings may have a major interest for the treatment of T2D and of its hepatic complications. We showed that metformin, the most widely prescribed oral insulin sensitizer agent, prevented the PDGF-AA insulin-induced vicious circle. Metformin has been specifically proposed for patients with diabetes with NAFLD and HCC (42). Metformin reduces the risk of HCC incidence in patients with diabetes in a dose-dependent manner (43). Metformin may thus improve liver insulin sensitivity at least partly through PDGF-AA liver blockade, explaining its long-term effect

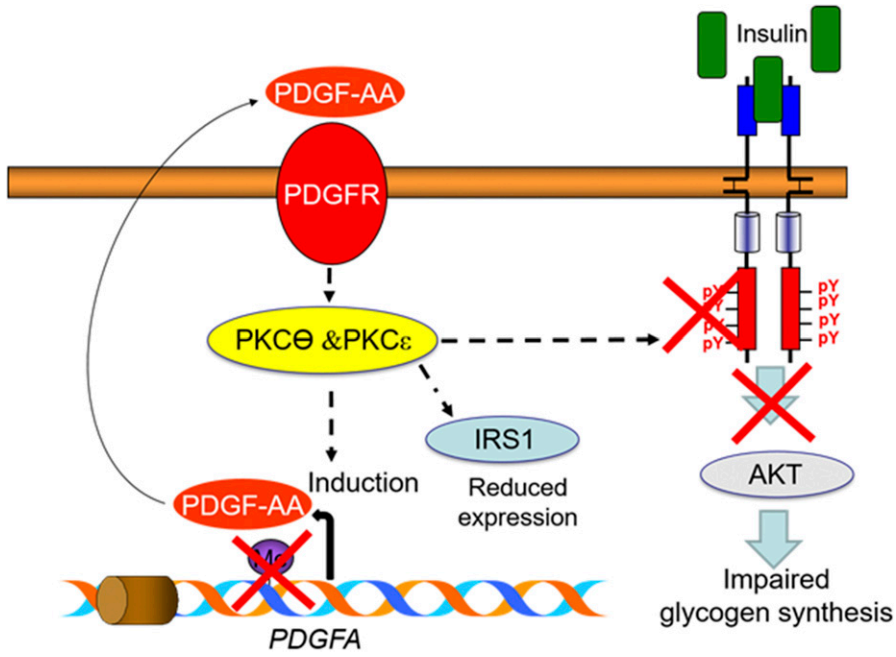

Figure 7—Schematic representation of the mechanism linking hyperinsulinemia to hepatic insulin resistance in T2D. Insulin promotes hypomethylation and the rise of *PDGFA* expression, leading to PDGF-AA secretion. In turn, PDGF-AA inhibits the insulin signaling in a negative autocrine feedback loop via a mechanism involving a decrease in the IRS1 and INSR abundance and PKCΘ and PKCε activation.

against HCC. Besides liver insulin sensitizers, blocking PDGF-AA activity may be a promising alternative to antidiabetic therapeutics. The antitumor PDGFR inhibitor imatinib demonstrated unexpected (and unexplained until now) improvement of insulin sensitivity in insulin-resistant rats (48) as well as a dramatic blood glucose–lowering effect in subjects with diabetes treated for leukemia (49,50).

Our study also suggests that human epigenome analysis, when directly performed in disease-affected tissues, is an efficient tool to make progress in the pathogenesis of common diseases. Furthermore, it opens avenues in the identification of new drug targets to combat T2D and complications linked to insulin resistance, including NAFLD and cancer.

Acknowledgments. The authors are grateful to Estelle Leborgne (Institut Pasteur de Lille) for helping in the illustrations of the manuscript.

Funding. This study was supported by nonprofit organizations and public bodies for funding of scientific research conducted in France and within the European Union: Centre National de la Recherche Scientifique, Université de Lille 2, Institut Pasteur de Lille, Société Francophone du Diabète, Contrat de Plan État-Région, Agence Nationale de la Recherche (ANR-10-LABX-46, ANR-10-EQPX-07-01), and H2020 European Research Council (GEPIDIAB - 294785).

Duality of Interest. No potential conflicts of interest relevant to this article were reported.

Author Contributions. A.A., L.Y., R.C., M.C., S.C., V.R., V.Pl., V.Pa., S.L., J.M., L.R., R.B., G.Q., M.K., M.T., J.B., S.S., E.A., P.J., J.D., O.S., I.R., A.L., M.P., M.D.-C., S.G.-C., T.D., G.L., P.M., B.S., J.A., A.S., C.P., C.S., J.H., A.B., F.P., and P.F. read and approved the final version of the manuscript. A.A., L.Y., M.C., A.B., and P.F. drafted and wrote the manuscript. A.A., L.Y., S.C., and P.F. designed the study. A.A., R.C., M.C., S.C., V.R., S.L., J.M., L.R., A.L., T.D., G.L., P.M., B.S., J.A., A.S., C.P., J.H., A.B., F.P., and P.F. revised the manuscript. L.Y. and M.C. performed statistical analyses. V.Pl., S.L., J.M., L.R., R.B., G.Q., M.K., M.T., J.B., S.S., E.A., P.J., J.D., A.L., M.D.-C., S.G.-C., and G.L. performed the experiments. O.S., I.R., and A.B. performed the bioinformatics analysis. A.A. and P.F. are the guarantors of this work and, as such, had full access to all the data in the study and take responsibility for the integrity of the data and the accuracy of the data analysis.

Prior Presentation. Parts of this study were presented in abstract form at the 77th Scientific Sessions of the American Diabetes Association, San Diego, CA, 9–13 June 2017.

A non–peer-reviewed version of this article was submitted to the arXiv preprint server (https://arxiv.org/abs/1712.04680) on 13 December 2017.

References

1. Stefan N, Häring H-U. The metabolically benign and malignant fatty liver. Diabetes 2011;60:2011–2017
2. Bonnefond A, Froguel P. Rare and common genetic events in type 2 diabetes: what should biologists know? Cell Metab 2015;21:357–368
3. Ling C, Groop L. Epigenetics: a molecular link between environmental factors and type 2 diabetes. Diabetes 2009;58:2718–2725
4. Kirchner H, Sinha I, Gao H, et al. Altered DNA methylation of glycolytic and lipogenic genes in liver from obese and type 2 diabetic patients. Mol Metab 2016;5:171–183
5. Muka T, Nano J, Voortman T, et al. The role of global and regional DNA methylation and histone modifications in glycemic traits and type 2 diabetes: a systematic review. Nutr Metab Cardiovasc Dis 2016;26:553–566
6. Nilsson E, Matte A, Perfilyev A, et al. Epigenetic alterations in human liver from subjects with type 2 diabetes in parallel with reduced folate levels. J Clin Endocrinol Metab 2015;100:E1491–E1501
7. Nilsson E, Jansson PA, Perfilyev A, et al. Altered DNA methylation and differential expression of genes influencing metabolism and inflammation in adipose tissue from subjects with type 2 diabetes. Diabetes 2014;63:2962–2976
8. Wahl S, Drong A, Lehne B, et al. Epigenome-wide association study of body mass index, and the adverse outcomes of adiposity. Nature 2017;541:81–86

9. Thieringer F, Maass T, Czochra P, et al. Spontaneous hepatic fibrosis in transgenic mice overexpressing PDGF-A. Gene 2008;423:23–28
10. Caiazzo R, Lassailly G, Leteurtre E, et al. Roux-en-Y gastric bypass versus adjustable gastric banding to reduce nonalcoholic fatty liver disease: a 5-year controlled longitudinal study. Ann Surg 2014;260:893–898; discussion 898–899
11. Ahrens M, Ammerpohl O, von Schönfels W, et al. DNA methylation analysis in nonalcoholic fatty liver disease suggests distinct disease-specific and remodeling signatures after bariatric surgery. Cell Metab 2013;18:296–302
12. Bibikova M, Barnes B, Tsan C, et al. High density DNA methylation array with single CpG site resolution. Genomics 2011;98:288–295
13. Voight BF, Kang HM, Ding J, et al. The Metabochip, a custom genotyping array for genetic studies of metabolic, cardiovascular, and anthropometric traits. PLoS Genet 2012;8:e1002793
14. Aryee MJ, Jaffe AE, Corrada-Bravo H, et al. Minfi: a flexible and comprehensive Bioconductor package for the analysis of Infinium DNA methylation microarrays. Bioinformatics 2014;30:1363–1369
15. Teschendorff AE, Marabita F, Lechner M, et al. A beta-mixture quantile normalization method for correcting probe design bias in Illumina Infinium 450 k DNA methylation data. Bioinformatics 2013;29:189–196
16. Samanez CH, Caron S, Briand O, et al. The human hepatocyte cell lines IHH and HepaRG: models to study glucose, lipid and lipoprotein metabolism. Arch Physiol Biochem 2012;118:102–111
17. Pichard L, Raulet E, Fabre G, Ferrini JB, Ourlin JC, Maurel P. Human hepatocyte culture. Methods Mol Biol 2006;320:283–293
18. Houseman EA, Kile ML, Christiani DC, Ince TA, Kelsey KT, Marsit CJ. Reference-free deconvolution of DNA methylation data and mediation by cell composition effects. BMC Bioinformatics 2016;17:259
19. Murphy SK, Yang H, Moylan CA, et al. Relationship between methylome and transcriptome in patients with nonalcoholic fatty liver disease. Gastroenterology 2013;145:1076–1087
20. Zeybel M, Hardy T, Robinson SM, et al. Differential DNA methylation of genes involved in fibrosis progression in non-alcoholic fatty liver disease and alcoholic liver disease. Clin Epigenetics 2015;7:25
21. Andrae J, Gallini R, Betsholtz C. Role of platelet-derived growth factors in physiology and medicine. Genes Dev 2008;22:1276–1312
22. Awuah PK, Nejak-Bowen KN, Monga SPS. Role and regulation of PDGFRα signaling in liver development and regeneration. Am J Pathol 2013;182:1648–1658
23. Hayes BJ, Riehle KJ, Shimizu-Albergine M, et al. Activation of platelet-derived growth factor receptor alpha contributes to liver fibrosis. PLoS One 2014;9:e92925
24. Liu X, Brenner DA. Liver: DNA methylation controls liver fibrogenesis. Nat Rev Gastroenterol Hepatol 2016;13:126–128
25. Kocabayoglu P, Lade A, Lee YA, et al. β-PDGF receptor expressed by hepatic stellate cells regulates fibrosis in murine liver injury, but not carcinogenesis. J Hepatol 2015;63:141–147
26. Scott RA, Lagou V, Welch RP, et al.; DIAbetes Genetics Replication and Meta-analysis (DIAGRAM) Consortium. Large-scale association analyses identify new loci influencing glycemic traits and provide insight into the underlying biological pathways. Nat Genet 2012;44:991–1005
27. Baumeier C, Saussenthaler S, Kammel A, et al. Hepatic DPP4 DNA methylation associates with fatty liver. Diabetes 2017;66:25–35
28. Wong NC, Ng J, Hall NE, et al. Exploring the utility of human DNA methylation arrays for profiling mouse genomic DNA. Genomics 2013;102:38–46
29. Shimomura I, Matsuda M, Hammer RE, Bashmakov Y, Brown MS, Goldstein JL. Decreased IRS-2 and increased SREBP-1c lead to mixed insulin resistance and sensitivity in livers of lipodystrophic and ob/ob mice. Mol Cell 2000;6:77–86
30. Gross SM, Rotwein P. Mapping growth-factor-modulated Akt signaling dynamics. J Cell Sci 2016;129:2052–2063
31. Mackenzie RW, Elliott BT. Akt/PKB activation and insulin signaling: a novel insulin signaling pathway in the treatment of type 2 diabetes. Diabetes Metab Syndr Obes 2014;7:55–64
32. Michelini E, Lonardo A, Ballestri S, et al. Is cholangiocarcinoma another complication of insulin resistance: a report of three cases. Metab Syndr Relat Disord 2007;5:194–202
33. Hilhorst R, Houkes L, Mommersteeg M, Musch J, van den Berg A, Ruijtenbeek R. Peptide microarrays for profiling of serine/threonine kinase activity of recombinant kinases and lysates of cells and tissue samples. *Methods Mol Biol* 2013;977:259–271
34. Dasgupta S, Bhattacharya S, Maitra S, et al. Mechanism of lipid induced insulin resistance: activated PKCε is a key regulator. Biochim Biophys Acta 2011;1812:495–506
35. Kim JK, Fillmore JJ, Sunshine MJ, et al. PKC-θ knockout mice are protected from fat-induced insulin resistance. J Clin Invest 2004;114:823–827
36. Samuel VT, Liu Z-X, Wang A, et al. Inhibition of protein kinase Cepsilon prevents hepatic insulin resistance in nonalcoholic fatty liver disease. J Clin Invest 2007;117:739–745
37. Cenni V, Döppler H, Sonnenburg ED, Maraldi N, Newton AC, Toker A. Regulation of novel protein kinase C epsilon by phosphorylation. Biochem J 2002;363:537–545
38. Liu Y, Graham C, Li A, Fisher RJ, Shaw S. Phosphorylation of the protein kinase C-theta activation loop and hydrophobic motif regulates its kinase activity, but only activation loop phosphorylation is critical to in vivo nuclear-factor-kappaB induction. Biochem J 2002;361:255–265
39. Evenou J-P, Wagner J, Zenke G, et al. The potent protein kinase C-selective inhibitor AEB071 (sotrastaurin) represents a new class of immunosuppressive agents affecting early T-cell activation. J Pharmacol Exp Ther 2009;330:792–801
40. Marra F, Choudhury GG, Pinzani M, Abboud HE. Regulation of platelet-derived growth factor secretion and gene expression in human liver fat-storing cells. Gastroenterology 1994;107:1110–1117
41. Rodríguez-Lirio A, Pérez-Yarza G, Fernández-Suárez MR, Alonso-Tejerina E, Boyano MD, Asumendi A. Metformin induces cell cycle arrest and apoptosis in drug-resistant leukemia cells. Leuk Res Treatment 2015;2015:e516460
42. Dyson JK, Anstee QM, McPherson S. Republished: non-alcoholic fatty liver disease: a practical approach to treatment. Postgrad Med J 2015;91:92–101
43. Bo S, Benso A, Durazzo M, Ghigo E. Does use of metformin protect against cancer in Type 2 diabetes mellitus? J Endocrinol Invest 2012;35:231–235
44. Anstee QM, Day CP. The genetics of NAFLD. Nat Rev Gastroenterol Hepatol 2013;10:645–655
45. Cofer ZC, Cui S, EauClaire SF, et al. Methylation microarray studies highlight PDGFA expression as a factor in biliary atresia. PLoS One 2016;11:e0151521
46. Boonjaraspinyo S, Boonmars T, Wu Z, et al. Platelet-derived growth factor may be a potential diagnostic and prognostic marker for cholangiocarcinoma. Tumour Biol 2012;33:1785–1802
47. Bril F, Lomonaco R, Orsak B, et al. Relationship between disease severity, hyperinsulinemia, and impaired insulin clearance in patients with nonalcoholic steatohepatitis. Hepatology 2014;59:2178–2187
48. Hägerkvist R, Jansson L, Welsh N. Imatinib mesylate improves insulin sensitivity and glucose disposal rates in rats fed a high-fat diet. Clin Sci (Lond) 2008;114:65–71
49. Breccia M, Muscaritoli M, Aversa Z, Mandelli F, Alimena G. Imatinib mesylate may improve fasting blood glucose in diabetic Ph+ chronic myelogenous leukemia patients responsive to treatment. J Clin Oncol 2004;22:4653–4655
50. Veneri D, Franchini M, Bonora E. Imatinib and regression of type 2 diabetes. N Engl J Med 2005;352:1049–1050